Experimental and Theoretical Study of The Structure / Properties Relationship of a Derivative of The Organic Compound Morpholine

M.Drissi[1], S.Soualmi[1], M.Moumene[1], A.Amcha[2], A.Chouaih[2]
[1]*Laboratory of synthesis and Catalysis, University of Tiaret, Algeria*
[2]*Laboratoryof Technology and Solid Properties, University of Mostaganem*
mokadrissi@gmail.com
saida.soualmi@univ-tiaret.dz
taki407@yahoo.com
aekamcha6@gmail.com
aek_chouaih@yahoo.fr

***Abstract*—In the title compound, C18H19NO3S, the Morpholine ring adopts a chair conformation. The Thiophene ring forms dihedral angles of 26.04 (9) and 74.07 (10) with the benzene ring and the mean plane of the Morpholine ring, respectively. The crystal structure of a new organic compound with the chemical formula $C_{18}H_{19}NO_3S$, was determined by X-ray diffraction and theoretical calculations to establish the configuration, stereochemistry and stable conformation of the molecule. The theoretical calculations werecarried out using the density functional theory (DFT) (B3LYP) with the bases 6-31G (d, p) and 6-311 (d, p).The molecular conformation is stabilized by an O—HN hydrogen bond. In the crystal, molecules are connected through C—HO hydrogen bonds, forming wave-like layers parallel to the ab plane, which are further linked into a three-dimensional network by C—H interactions involving the benzene rings and the methylene H atoms of the morpholine rings. For highlighting the intra- and intermolecularchargetransfer nature, the molecular electrostatic potential has been analyzed. The molecular dipole moments were calculated and compared with those obtained using theoretical calculations. The NLO behavior of the title compound was examined by computing the molecular polarizabilities α andβ.**

***Index Terms*—Chalcones ; Crystal structure; Electron density (ED);DFT;NLO; HOMO; LUMO.**

I.INTRODUCTION

CHALCONES, *viz*1,3-diaryl-2-propene-1-ones, are major component of many natural products as well as important precursors for many synthetic manipulations [1-4]. Chalcones and their synthetic analogues display a wide range of biological activities such as anticancer, antimalarial, antibacterial, anti- inflammatory, antifungal, antioxidant, anti-*HIV*, anti- protozoal, and carbonic anhydrase inhibiting activities [5,8].

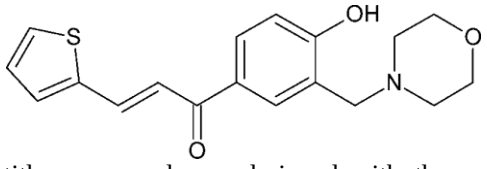

The title compound was designed with the expectation of observing an increased bioactivity or cyto-toxicity in a molecule including both chalconeand Mannich base pharmakophores[9].

II.EXPERIMENTAL CALCULATIONS

Crystal data, data collection and structure refinement details are summarized in Table 1. C-bound H atoms were placed in calculated positions with C—H = 0.93–0.97 A˚ and refined using a riding model with Uiso(H) = 1.2Ueq(C). The hydroxy H atom was found in a difference-Fourier map and refined with Uiso(H) = 1.5Ueq(O).

In the title compound (Fig. 1), the molecular conformation is enforced by an intramolecular O—HN hydrogen bond (Table 2) and the amine N atoms of the morpholine rings and the hydroxy groups of the phenol fragments are engaged in intramolecular hydrogenbonds.

"This work was supported in part by the 1st National Conference on Synthesis and Catalysis, Tiaret (CNSCT, 2021)

M. Drissi is with the Department of Chemistry, University of Tiaret.14000, (e-mail: mokhtaria.drissi@univ-tiaret.dz).

S. Soualmi is with the Department of Chemistry, University of Tiaret, (e-mail: saida.soualmi@univ-tiaret.dz).

M.Moumeneis with the Department of Chemistry, University of Tiaret.14000.(e-mail: taki407@yahoo.com

A. Chouaih is with Department of Chemistry; University of Mostaganem27000 (e-mail: Abdelkader.chouaih@univ-mosta.dz).

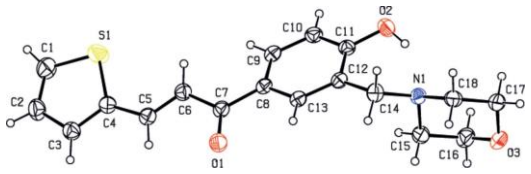

A. Multipolar Experimental Refinement

Electron density (ED) analysis has been carried out using Hansen-Coppens multipolar atom model [10]. The refinements were performed using MoPro package software [11]. The Hansen-Coppens multipolar refinement enables modeling of the non-spherical fraction of the atomic ED using the atom-centered multipole functions as described by following equation:

$$\rho_{atom}(\vec{r}) = \rho_c(\vec{r}) + P_V K'^3 \rho_v(K\vec{r}) + \sum_{l}^{lmax} \sum_{m=-1}^{+1} K''R_l(K''\vec{r}) P_{lm} Y_{lm}\left(\frac{\vec{r}}{r}\right)$$

Where: $\rho_c$and ρ_v are normalized spherically averaged free-atom core and valence densities, respectively; $(\kappa'\zeta r^{\rightarrow})$ is a Slater-type radial function and $dl(\theta,\phi)$ are density normalized real spherical harmonic functions. The populations Pv and Plmp, and the dimensionless expansioncontraction parameters κ and κ′ are refined against experimental data, while the population Pc of the core shell remains fixed. ζparameter is described by Hansen-Coppens model. In this work, multipolar refinement equation was developed to the third order (lmax = 3). The radial function coefficients for H-atoms were n1 = l and n1 = 2 and 3 for non–H atoms. Scattering factors for non–H atoms have been taken from the international tables for X-ray crystallography [12] and for the H-atoms Stewart data were used [13]. During the refinement, isotropic extinction correction has been applied and chemical constraints were imposed in order to limit the number of variables [14]. In parallel, the topological parameters and the molecular dipole moment of the title compound were also estimated. For highlighting the intra- and intermolecular charge transfer nature, the molecular electrostatic potential has been analyzed. All experimental ED deformation and electrostatic potential maps were plotted using the Moporo Viewer program [15]. Crystallographic details and refinement data are summarized in Table 1.

Table 1: Experimental details

Crystal data				
Chemical formula	$C_{18}H_{19}NO_3S$			
Chemical formula weight	329.40			
Cell setting	Monoclinic			
Space group	$P2_1/n$			
a (Å)	9.4939 (5))			
b (Å)	18.5548 (10)			
c (Å)	9.5068 (5)			
β(°)	96.788 (3)°			
V (Å³)	1662.95 (15)			
Z	4			
Radiation type	Mo *Kα*			
Wavelength (Å)	0.71073			
No. of reflections for cell parameters	25			
Temperature (K)	293(1)			
Data collection				
Diffractometer	Nonius CAD-4			
Data collection method	*θ* - 2*θ*			
*θ*max, *θ*min	28.5°, 2.2°			
No. of measured reflections	33902			
No. of independentreflections	4168			
No. of observed reflections	3373			
Criterion for observed reflections	$I \geq 2\sigma(I)$			
R_{int}	0.033			
Refinement				
	N	*R*	*wR*	*S*
Spherical refinement	92	0.038	0.040	1.02
Multipole refinement	221	0.022	0.035	1.12

N is the number of refined parameters and *M* is the number of observations. $R = \sum||F_o| - |F_c|| / \sum|F_o|$;

$wR = \left[\sum w(|F_o| - |F_c|)^2 / \sum w|F_o|^2\right]^{1/2}$; $S = \left[\sum w(|F_o| - |F_c|)^2 / (M - N)\right]^{1/2}$

III. THEORETICAL CALCULATIONS

A quantum-chemical calculation was performed using the *CNDO* (Complete Neglect of Differential Overlap) approximation of the program Gaussian [16-17]. The charges at atoms S1, O1, O2, O3 and N1 are -0.049, -0.336, -0.271, -0.224 and -0.145 e^-,respectively.

In addition, the geometrical optimization calculations of the title compound were performed using the *PM3* (Parameterized Model number3) method in *WinMopac7.2*.AviewofthemoleculecalculatedwithPM3is shown in Fig. 2. The net charges at atoms S1, O1, O2, O3 and N1 are -0.321,-0.230, -0.260, -0.321 and-0.070 e^-,respectively.

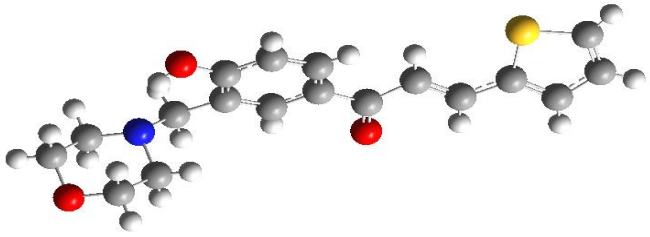

Figure2: Numbering of atoms for the title crystal: optimized structure

IV. RESULTS AND DISCUSSION

IV.1. Topological analysis of ED

Topological analysis of the experimental ED was performed with Mopro program. The equation used to calculate the final ED deformation map is:

$$\Delta(\vec{r}) = \rho_{mult}(\vec{r}) - \rho_{sph}(\vec{r})$$

$$=1/V\sum[|F_{mul}(\vec{r})e^{i\varphi mul(\vec{r})}-|Fsph(\vec{r})e^{i\varphi sph(\vec{r})}]e^{-i2\pi H\vec{}\cdot r\vec{}}$$

Multipole structure factors $Fmul(\vec{r})$ were used to obtain this map, where $Fsph(\vec{r})$ is evaluated from high-order refinement. The experimental ED deformation maps are shown in Figure 5 with contour map of 0.05 e.Å^{-3}. As can be noticed in Figure 5, the density peaks appear on all the chemical bonds. Figure 5(a) shows the ED in the benzene ring containing atoms form C9 to C14. It can be seen that the ED distribution is practically located on the chemical bonds. Furthermore, symmetrical distribution of electrons along C18-N1 and C15-N1 bonds shows clearly the multi connecting part (triple bond). Figure 5(b) shows the electron density distribution with advanced contours for the same cycle in which are observed the lone-pair charge concentrations of N atoms. To more study the electron density of cyano groups, we have explored a second plane perpendicular to the aromatic ring attached these groups, as can be seen in Figures 5(c) and 5(d). It is noted that the triple bond between the nitrogen and the carbon is rich in electrons due to the valence electrons of nitrogen atoms.

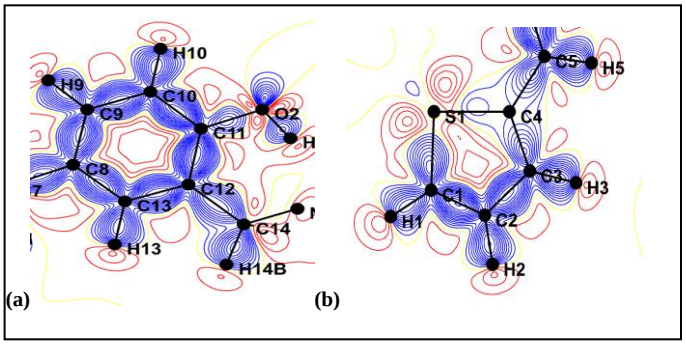

Figure 5: Deformation ED maps. Contour map of 0.05 e.Å-3. The blue coulour indicate the positive density and the red negative density: (a) Six-membered ring (C9-C14),(b): Ring (S-C1-C2-C3-C4) of thiophenwith advanced contour).

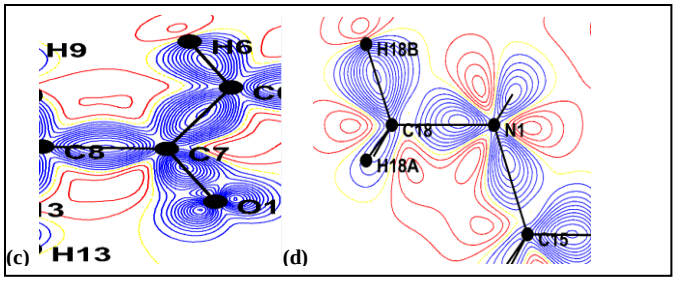

Figure 5: Deformation ED maps. Contour map of 0.05 e.Å-3. The blue coulour indicate the positive density and the red negative density: tours, (c): AroundC7=O1 bond, (d) Around C18-N1 and C15-N1 bonds).

Tableau III.1. Charges nettes (q) pour les différents atomes du composé

Atome	P_{val}	q (unité)	q_{thee}
C1	4.054	-0.054	-0.426
H1	0.920	0.08	0.171
C2	4.054	-0.054	-0.022
H2	0.920	0.08	0.167
C3	4.002	-0.002	-0.098
H3	0.920	0.08	0.208
C4	4.002	-0.002	-0.482
S	6.120	-0.120	0.501
C5	4.054	-0.054	-0.133
H5	0.920	0.08	0.173
C6	4.054	0.054	-0.127
H6	0.055	0.945	0.186
C7	4.113	-0.113	0.271
O1	6.226	-0.226	-0.398
C8	3.938	0.062	-0.236
C9	4.054	-0.054	-0.056
H9	0.920	0.08	0.172
C10	4.054	-0.054	-0.037
H10	0.920	0.08	0.193
C11	4.023	-0.023	0.030
O2	6.258	-0.258	-0.631
H	0.814	0.186	0.380
C12	4.041	-0.041	-0.159
C13	4.054	-0.054	0.249
H13	0.920	0.08	0.167
C14	3.865	0.135	-0.251
$H14_a$	0.974	0.026	0.177
$H14_b$	0.974	0.026	0.176
C15	3.865	0.135	-0.177
$H15_a$	0.974	0.026	0.161
$H15_b$	0.974	0.026	0.183
C16	3.891	0.109	-0.164
$H16_a$	0.990	0.01	0.176
$H16_b$	0.990	0.01	0.171
N	5.212	-0.212	-0.533
O3	6.239	-0.239	-0.425
C17	3.891	0.109	-0.135
$H17_a$	0.990	0.01	0.162
$H17_b$	0.990	0.01	0.201
C18	3.865	0.135	-0.131
$H18_a$	0.974	0.026	0.168
$H18_b$	0.974	0.026	0.174

IV.2. Electrostatic potential

Generally, the electrostatic potential (ESP) may be obtained from X-ray diffraction data or by quantum chemical calculation using theoretical methods. Hence, reactive areas for nucleophilic and electrophilic attacks can be predicted by ESP determination. For our molecule, as can be seen in Figure 9(a) , the ESP map provided by the multipolar refinement is plotted on an ED isosurface. Figure 9(b) shows the theoretical ESP map computed with DFT/B3LYP/6-31G(d,p) level of theory. As can be noted, experimental and theoretical results are wholly similar. From these results and as expected, oxygen and nitrogen atoms, namely O1, O2, N1, N2 and N3, constitute the most electronegative region which are favorable

sites for electrophilic attack. Whereas, the aromatic carbon and hydrogen atoms represent the electropositive region implying that these areas are favorable sites for nucleophilic attack.

Figure 7: Electrostatic potential map: (a) experimental, (b) theoretical)

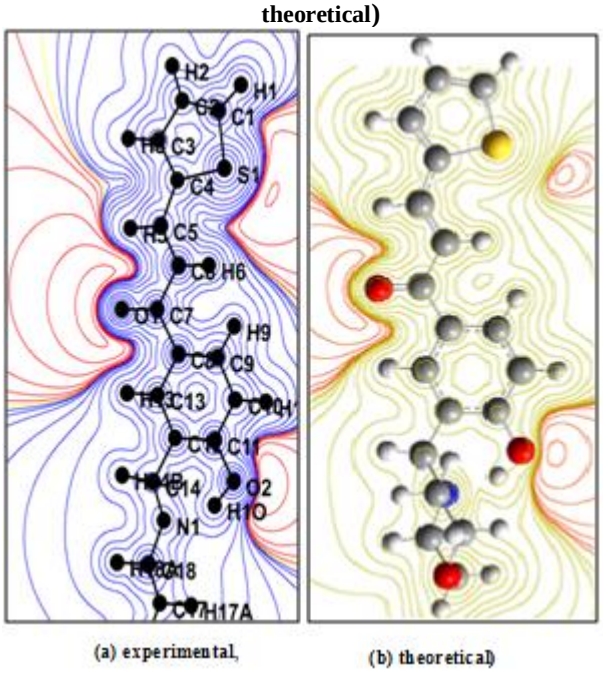

IV.3. Non-linear optical properties

For organic NLO materials, the origin of nonlinear behavior has been studied by conducting theoretical and experimental studies [19]. Theoretical calculation plays a significant role in understanding the structure-property relationship which is able to help in designing novel NLO materials. In this context and to understand this phenomenon regarding the investigated molecule, we have seen that it is indispensable to extend this study to the determination of the polarizability α and the first hyperpolarizabilityβ. NLO computations were accomplished with the help of quantum chemical methods in particular Hartree-Fock (HF), density functional theory (DFT/B3LYP) and Møller-Plesset (MP2), using 6-31G(d,p) basis set. In addition, PM6 semi-empirical method was used for comparison. The following conventional equations were used to estimate the isotropic polarizability (α) and the first hyperpolarizability (β) tensors:

$$\mu=(\mu_x^2+\mu_y^2+\mu_z^2$$

$$\alpha_{tot}=\frac{a_{xx}+a_{yy}+a_{zz}}{3}$$

The whole equation for computing β magnitude is given below:

$\beta_{tot} = (\beta_x^2 + \beta_y^2+\beta_z^2)^{1/2}$

With

$$\beta_x = \beta_{xxx} + \beta_{xyy} + \beta_{xzz}$$

$$\beta_y = \beta_{yyy} + \beta_{xxy} + \beta_{yzz}$$

$$\beta_z = \beta_{zzz} + \beta_{xxz} + \beta_{yyz}$$

As β is depicted by a 3×3×3 matrices and using symmetry reported by Kleinman[20], the 3D matrix is reduced to 10 components which are provided by Gaussian program output. These tensors are given in atomic units (a.u) and were converted into electrostatic units. (α: 1 au = 0.1482×10^{-24}esu ; β: 1 au = 8.6393×10^{-33}esu).

Usually, the ONL activity is directly related to the values of polarizability and hyperpolarizability. The calculated polarizability (α) obtained with B3LYP/6-31G(d,p) basis set is equal to 4.16×10^{-23}esu. As it can be seen from results, the diagonal components are dominant in the computed α_{ij}tensors. The most important β value of the title molecule is about 28.60×10^{-30}esu calculated with B3LYP/6-31G(d,p). Thus, computed low β value for the title molecule (7.92×10^{-30}esu obtained at HF/6-31G(d,p)) compared to that of urea (0.1947×10^{-30}esu) is about 40 times. Therefore, these results indicate that the title molecule have significant NLO comportment.

Table 4 :Polarizabilty (α) and hyperpolarizability (β) values of the C21H13N3O2 molecule obtained by HF, DFT/B3LYP and MP2 methods using 6-31G(d,p) basis set along with the PM6 semi-empirical method.

	HF/6-311G+(d)	**DFT/6-311G+(d)**
α_{xx}	357.420	422.543
α_{xy}	-9.815	-9.475
α_{yy}	204.781	216.255
α_{xz}	23.881	25.367
α_{yz}	-0.826	-0.144
α_{zz}	126.680	132.133
α (u.a)	**229.627**	**770.931**
α×10^{-23} (esu)	**3.403**	**11.425**
β_{xxx}	-242.318	261.078
β_{xxy}	-840.092	-1118.548
B_{xyy}	181.143	402.114
B_{yyy}	12.098	-85.267
B_{xxz}	-93.348	-121.309
B_{xyz}	-45.399	-34.968
β_{yyz}	22.997	28.164
β_{xzz}	-26.571	22.832
β_{yzz}	2.932	-46.150
β_{zzz}	-29.225	-54.503
β (u.a)	**835.668**	**1437.795**
β×10^{-30} (esu)	**7.219**	**12.421**

IV.4. Frontier molecular orbital analysis

Molecular orbitals (HOMO-LUMO) and their properties such as energy are very useful for physicist and chemists and are very important parameters for quantum chemistry. This is also used by the frontier electron density for predicting the most reactive position in π-electron systems and also explains several types of reaction in conjugated system [21-22]. The conjugated molecules are characterized by a small highest occupied molecular orbital- lowest unoccupied molecular

orbital (HOMO-LUMO). Both the highest occupied molecular orbital and lowest unoccupied molecular orbital are the main orbitals which take part in chemical stability. The HOMO and LUMO energy calculated by B3LYP/6-311++G(d,p) method is shown below. This electronic absorption corresponds to the transition from the ground to the first excited state and is mainly described by one electron excitation from the highest occupied molecular orbital to the lowest unoccupied molecular orbital. While the energy of the HOMO describe the ionization potential, LUMO energy is concerned by the electron affinity Energy difference between HOMO and LUMO orbital is called as energy gap which is an important stability for structures [23-24]. Recently, it has been shown that calculated energy gap between HOMO and LUMO can be very useful to prove the activity from intramolecular charge transfer. The plots of HOMO and LUMO are shown in figure-5.

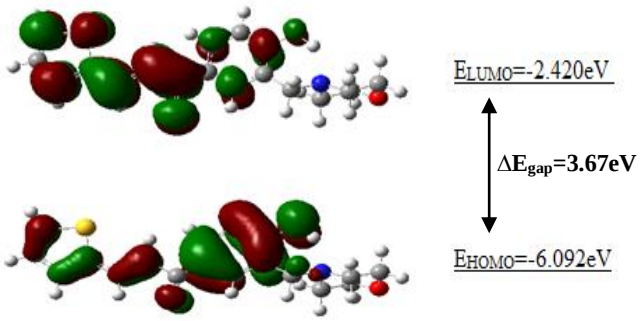

Figure 8: Plots of HOMO and LUMO of (2E)-1-[4-hydroxy-3-(morpholin -4-ylmethyl)-phenyl]-3-(thiophen-2-yl)prop-2-en-1-one

V. 5Conclusions

The experimental charge density of (2E)-1-[4-hydroxy-3-(morpholin -4-ylmethyl)-phenyl]-3-(thiophen-2-yl)prop-2-en-1-onewas investigated by means of multipolar refinement using single crystal X-ray diffraction data collected at low temperature. Directional C–H···O and O–H···N intermolecular interactions have been highlighted using Hirshfeld surface analysis. The close contacts with their individual contributions were established by the fingerprint plots. The high quality of the ED is confirmed by the accumulation of deformation densities on the chemical bonds obtained from multipolar refinement. In order to investigate the electrostatic behavior of the crystal, the X-ray charge density study was carried out. The experimental electrostatic potential was determined and compared to that computed using DFT method. In addition, ESP maps show that the hydrogen atoms represent the positive potential regions while the electronegative atoms constitute the negative potential regions. Negative and positive regions in the molecule are very important for establishing intra- and intermolecular contacts. Nonlinear optical properties have been calculated using computational methods. This study reveals that the title molecule has a significant hyperpolarizability and can be used to develop NLO materials. Finally, structural details, topological, electrostatic and NLO properties reported in this study can be helpful for phthalonitrile derivatives designing.

REFERENCES

[1] Das, U., Gul, H. I., Alcorn, J., Shrivastav, A., George, T., Sharma,R. K., Nienaber, K. H., De Clercq, E., Balzarini, J., Kawase, M.,Kan, N., Tanaka, T., Tani, S., Werbovetz, K. A., Yakovich, A. J.,Manavathu, E. K., Stables, J. P. &Dimmock, J. R. Eur. J.Med. Chem. 41, 577–585. 2006.

[2] Yerdelen, K. O., Gul, H. I., Sakagami, H., Umemura, N. &Sukuroglu, M. Lett. Drug. Des. Discov. 12, 643–649. 2015.

[3] Gul, H. I., Cizmecioglu, M., Zencir, S., Gul, M., Canturk, P., Atalay, M. &Topcu, Z. J. Enzyme Inhib. Med. Chem. 24, 804–807.2009.

[4] Gul, H. I., Yerdelen, K. O., Gul, M., Das, U., Pandit, B., Li, P.-K., Secen, H. &Sahin, F.2007. Arch. Pharm. Chem. Life Sci. 340, 195–201. 2007.

[5] Bilginer, S., Unluer, E., Gul, H. I., Mete, E., Isik, S., Vullo, D., Ozensoy-Guler, O., Beyaztas, S., Capasso, C. &Supuran, C. T. (2014). J. Enzyme Inhib. Med. Chem. 29, 495–499.

[6] Bilginer, S., Gul, H. I., Mete, E., Das, U., Sakagami, H., Umemura, N.&Dimmock, J. R. (2013). J. Enzyme Inhib. Med. Chem. 28, 974–980.

[7] Singh, P., Anand, A. & Kumar, V. Eur. J. Med. Chem. 85, 758–777. 2014.

[8] Yamali, C., Tugrak, M., Gul, H. I., Tanc,M. &Supuran, C. T.. J.EnzymeInhib. Med. Chem. 31, 1678–1681. 2016.

[9] FatmaYesilyurt,a Abdullah Aydin,b* HaliseInciGul,a Mehmet Akkurtc andNefiseDilekOzcelikd.Acta Cryst. E74, 960–963.2018.

[10] M. Drissi A. Chouaih, Y. Megrouss, F. Hamzaoui, Journal of Crystallography, **2013**,ID 326457.2013.

[11] C. Jelsch, B. Guillot, A. Lagoutte, C. Lecomte, J. Applied Crystallography 38, 38.2005.

[12] E. Prince, A. J. C. Wilson, International Tables for X-Ray Crystallography, vol. C,2nd edition, Kluwer Academic, Boston, Mass, USA, 1999.

[13] R. F. Stewart, E. R. Davidson, W. T. Simpson, The Journal of Chemical Physicsvol. 42(9),3175.1965.

[14] P. Coppens, X-Ray Charge Densities and Chemical Bonding, Oxford, NewYork, NY, USA,1997.

[15] B. Guillot, ActaCryst. A 68, 204.2012.

[16] M.J. Frisch , G.W. Trucks , H.B. Schlegel , G.E. Scuseria , M.A. Robb , J.R. Cheese-man , G. Scalmani , V. Barone , B. Mennucci , G.A. Petersson , H. Nakatsuji , M. Caricato , X. Li , H.P. Hratchian , A.F. Izmaylov , J. Bloino , G. Zheng , J.L. Son-nenberg , M. Hada , M. Ehara , K. Toyota , R. Fukuda , J. Hasegawa , M. Ishida , T. Nakajima , Y. Honda , O. Kitao , H. Nakai , T. Vreven , J.A. Montgomery Jr. , J.E. Peralta , F. Ogliaro , M. Bearpark , J.J. Heyd , E. Brothers , K.N. Kudin , V.N. Staroverov , T. Keith , R. Kobayashi , J. Normand , K. Raghavachari , A. Ren- dell , J.C. Burant , S.S. Iyengar , J. Tomasi , M. Cossi , N. Rega , J.M. Millam , M. Klene , J.E. Knox , J.B. Cross , V. Bakken , C. Adamo , J. Jaramillo , R. Gom- perts , R.E. Stratmann , O. Yazyev , A.J. Austin , R. Cammi , C. Pomelli , J.W. Ochter- ski , R.L. Martin , K. Morokuma , V.G. Zakrzewski , G.A. Voth , P. Salvador , J.J. Dannenberg , S. Dapprich , A.D. Daniels , O. Farkas , J.B. Foresman , J.V. Ortiz , J. Cioslowski , D.J. Fox , Gaussian 09, Revision B.01, Gaussian, Inc., Wallingford CT, 2009.

[17] R. Dennington. T. Keith. J. Millam: SemichemInc, Shawnee Mission KS. GaussView. Version 5, 2009.

[18] D. Sajan, H. J. Ravindra, M. Neeraj, I. Hubert Joe, Vibrational Spectroscopy **54**, 72.2010.

[19] C. Jelsch, B. Guillot, A. Lagoutte, C. Lecomte, J. Applied Crystallography **38**, 38 (2005).

[20] R.S. Mulliken, A New Electroaffinity Scale; Together with Data on Valence States and on Valence Ionization Potentials and Electron Affinities, J. Chem. Phys. 2 . 782.1934.

[21] D. A. Kleinman, Phys. Rev. **126**, 1977 (1962).

[22] R.G. Pearson, Absolute electronegativity and hardness: applications to organic chemistry, J. Org. Chem. 54.1423. 1989.

[23] [51] R.G. Pearson, Chemical Hardness-Applications from Molecules to Solids, John Wiley–VCH, Weinheim, 1997.

[24] N.E.H. Belkafouf, F. Triki-Baara, A. Altomare, R. Rizzi, A. Chouaih, A. Djafri, F. Hamzaoui, Synthesis, PXRD structural determination, Hirshfeld surface analysis and DFT/TD-DFT investigation of 3N-ethyl-

2N'-(2-ethylphenylimino) thiazolidin- 4-one, J. Mol. Struct. 1189 . 8–
20. 2019..